16-osios jaunųjų mokslininkų konferencijos „Mokslas – Lietuvos ateitis“ teminės konferencijos
TRANSPORTO INŽINERIJA IR VADYBA,
vykusios 2013 m. gegužės 8 d. Vilniuje, straipsnių rinkinys

Proceedings of the 16th Conference for Junior Researchers ‘Science – Future of Lithuania’
TRANSPORT ENGINEERING AND MANAGEMENT, 8 May 2013, Vilnius, Lithuania

Сборник статей 16-й конференции молодых ученых «Наука – будущее Литвы»
ИНЖЕНЕРИЯ ТРАНСПОРТА И ОРГАНИЗАЦИЯ ПЕРЕВОЗОК, 8 мая 2013 г., Вильнюс, Литва

COMPUTER TECHNOLOGIES OF FINITE ELEMENT MODELLING OF AIRFIELD RIGID PAVEMENT

Olexander Rodchenko
National Aviation University, Kyiv, Ukraine
E-mail: s140983t@bigmir.net

Abstract. Finite element modelling of airfield two-layer rigid pavement can be provided in program LIRA. FEM programs FEAFAA, FAARFIELD, ILLI-SLAB, ABAQUS do not provide finite element model of two-layer concrete pavement on the stabilized base. The maximum bending moment of upper slab computed by LIRA is more than the bending moment computed by SNiP. Finite element model of multi-slab jointed two-layer rigid pavement for program LIRA allows analyzing pavement with or without separator layer and under impact of new large aircrafts all main landing gears.

Keywords: finite element method, airfield rigid pavement, main landing gear, dower bar, joint, separator layer, compression ratio.

Introduction

In Ukraine conventional airfield rigid pavement of the international airports is two-layer concrete pavement on the stabilized base that’s why finite element analysis is important for airfield rigid pavement design under impact of the main landing gears of new large aircrafts (A380, B747-8).

There are different programs for airfield rigid pavement finite element analysis such as FEAFAA, FAARFIELD, ILLI–SLAB, ABAQUS but they do not provide finite element model of two-layer concrete pavement on the stabilized base that’s why the finite element method (FEM) software LIRA has been selected for that purpose.

1. FEM software

FEAFAA (Finite Element Analysis – Federal Aviation Administration) was developed by the FAA Airport Technology R&D Branch as a stand-alone tool for three-dimensional (3D) finite element analysis of multiple-slab airfield rigid pavements. It is useful for computing accurate responses (stresses, strains and deflections) of rigid pavement structures to individual aircraft landing gear loads. The major features of FEAFAA are: from single- to nine-slab jointed rigid pavement model, infinite subgrade model and arbitrary gear loading capability (Hammons 1998).

FAARFIELD (Federal Aviation Administration Rigid and Flexible Iterative Elastic Layered Design) designs the slab thickness based on the assumption of edge loading. The gear load is located either tangent or perpendicular to the slab edge, and the larger of the two stresses, reduced by 25 percent to account for load transfer through the joint, is taken as the design stress for determining the slab thickness. The program computes only the thickness of the concrete layer. The major features of FAARFIELD are: 1-slab rigid pavement model, infinite subgrade model, arbitrary gear loading capability, failure model.

ILLI-SLAB (Illinois Slab) is the two-dimensional (2D) finite element analysis (FEA) program. It provides nine slabs with joints. Two-dimensional shell finite elements are used to represent slab layer. Subgrade model is represented by Winkler’s hypothesis (Roesler 2007). User

ISSN 2029-7157 / eISSN 2029-7149
ISBN 978-609-457-490-0 / eISBN 978-609-457-489-4

cannot create two-layer slab on the conventional (sand or crushed aggregate) or stabilized base.

Abaqus FEA (formerly ABAQUS) is the general purpose finite element program. One of the salient features of Abaqus FEA is its use of the library concept to create different models by combining different solution procedures, element types, and material models (Brill 1998).

LIRA (it is not abbreviation) is the general purpose finite element program that was developed in Kyiv (Ukraine).

2. Finite element modelling of joints

A rigid pavement system consists of a number of Portland cement concrete (PCC) slabs finite in length and width over one or more base and subbase layers. When a slab is subjected to a wheel load, it develops bending stresses and distributes the load over the base. However, the response of these finite slabs is controlled by joint. Two methods are used to provide load transfer across concrete pavement joints – aggregate interlock and dowels. Aggregate interlock joints are formed during pavement construction by sawing 1/3 of the way through the pavement. Dowels are smooth rods, generally plainer epoxy-coated steel, which are usually oiled on side to allow the joints to open and close without resistance.

Finite element modelling of airfield rigid pavement can be provided in program LIRA that is the general purpose finite element method software. Multiple-slab jointed rigid pavement model includes nine slabs that are illustrated in Fig. 1. Longitudinal joint of pavement can include aggregate interlock or tie bars. Transverse joint include dowel bars. Joints between adjacent slabs are spring connection. The ideal spring connection would be one that provides a vertical spring force proportional to the relative vertical displacement between adjacent slab edges but does not constrain movement in any other direction (Fig. 2).

For an aggregate interlock load transfer mechanism, the joint stiffness is prescribed by the parameter *k*, which defines the force transmitted per unit length along the joint per unit differential deflection across the joint. For the dowel load transfer mechanism, *k* is defined as (Hammons 1998).

$$k = \frac{D}{s}, \tag{1}$$

where: *s* is the dowel spacing.

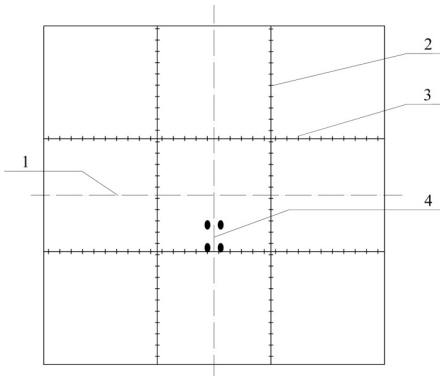

Fig. 1. Nine-slab jointed rigid pavement model: 1 – Portland cement concrete slab; 2 – longitudinal joint with aggregate interlock or tie bars; 3 – transverse joint with dowel bars; 4 – wheel loading (aircraft main landing gear)

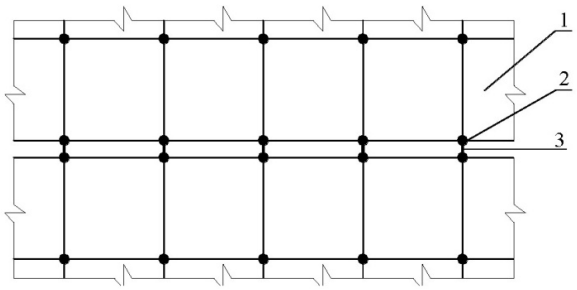

Fig. 2. Joint finite element model: 1 – shell finite element; 2 – node; 3 – FE 55

The value of *D* depends upon the vertical stiffness caused by the support of the concrete, called the dowel-concrete interaction *(DCI)*, and a vertical stiffness caused by beam bending. These two spring stiffnesses are summed as springs in series as follows (Hammons 1998):

$$D = \frac{1}{\frac{1}{DCI} + \frac{1}{12C}}. \tag{2}$$

The value of *DCI* is based on assuming the dowel to be a beam on a spring foundation and is given by the following relationship (Hammons 1998):

$$DCI = \frac{4\beta^3}{(2 + \beta\omega)} E_d I_d, \tag{3}$$

where: ω is the width of the joint opening, m; E_d is Young modulus (elasticity modulus), MPa; I_d is the dowel inertia moment, m^4.

The term β is identical to that used by Friberg (Hammons 1998)

$$\beta = \sqrt[4]{\frac{Kd}{4E_d I_d}}, \tag{4}$$

where: *K* is the modulus of dowel support, MN/m^3; d is the dowel diameter, m.

The term C in equation (2) is defined by the relationship (Hammons 1998):

$$C = \frac{E_d I_d}{\omega\left(1 + \frac{12 E_d I_d}{G_d A_z \omega^2}\right)}, \quad (5)$$

where: G_d is the shear modulus of the dowel bar, MPa; A_z is the effective cross-sectional area in shear, m^2.

The shear modulus of the dowel bar G_d is defined by (Hammons 1998):

$$G_d = \frac{E_d}{2(1+\mu_d)}, \quad (6)$$

where: μ_d is Poisson's ratio.

The term A_z is the effective cross-sectional area in shear and is assumed to be 0.9 times the circular area as follows (Hammons 1998):

$$A_z = 0{,}9\frac{\pi d^2}{4}. \quad (7)$$

Once k has been established, it is necessary to distribute the stiffness to the nodes along the joint in a rational manner. One method of allocating the stiffness to the nodes is by using the concept of contributing area, which is commonly used in structural analysis. In this method the stiffness values assigned to each node, R_Z (stiffness of FE 55), are determined based upon the length that contributes to the stiffness of the node. For equally spaced nodes in a 2D model, the nodes along a joint may be categorized into one of two types: interior nodes and edge nodes. Edge nodes are those which occupy the ends of the joint, while all other nodes are interior nodes. Based upon the concepts of contributing area, the stiffness of the interior nodes R_z must be twice that of the edge nodes $R_{z,e}$. If the length of the joint is given by L, and the number of nodes along the joint is given by n, then:

$$R_Z = \frac{kL}{(n-1)}, \quad (8)$$

$$R_{Z,e} = 0{,}5 \cdot R_Z. \quad (9)$$

where: L is the length of the joint, n is the number of nodes along the joint.

For unequally spaced nodes in a 2D model the stiffness of the interior nodes R_z is defined as:

$$R_{Z,un} = \frac{(a_{i-1} + a_{i+1})(n-1)}{2L} \cdot R_Z, \quad (10)$$

where: a_{i-1}, a_{i+1} are spaces between nodes, m.

3. Finite element modelling of two-layer rigid pavement

Two-dimensional shell finite elements are used to represent the upper and lower concrete slab of two-layer rigid pavement and stabilized base. Subgrade model is Winkler foundation.

The upper and lower concrete slabs are unbounded layers with or without the separator layer. Polyethylene sheeting, thin chip seal or slurry seals can be used as separators.

Compression of interacting layers of multi-layer rigid pavement is described by compression ratio. If the separator layer is located between rigid pavement layers compression ratio is defined by (Totskyi *et al.* 1982):

$$C_i = \frac{2{,}4 \cdot E_i E_{i+1} E}{E \cdot (h_i E_{i+1} + h_{i+1} E_i) + 2{,}4 \cdot E_i E_{i+1} h \mu_1}, \quad (11)$$

where: E_i, E_{i+1} are the elasticity moduluses of a rigid pavement layers, MPa; E is the elasticity modulus of the separator layer, MPa; h_i, h_{i+1} are the thicknesses of a rigid pavement layers, m; h is the thickness of the separator layer, m; μ_1 is the reduced Poisson's ratio of the separator layer.

The reduced Poisson's ratio of the separator layer is defined by the relationship (Totskyi *et al.* 1982):

$$\mu_1 = 1 - \frac{2\mu^2}{1-\mu}, \quad (12)$$

where: μ is Poisson's ratio of the separator layer.

For two-layer rigid pavement equation (11) is as follow:

$$C_p = \frac{2{,}4 \cdot E_{up} E_l E}{E \cdot (h_{up} E_l + h_l E_{up}) + 2{,}4 \cdot E_{up} E_l h \nu_1}, \quad (13)$$

where: E_{up} is the elasticity modulus of upper layer, MPa; E_l is the elasticity modulus of lower layer, MPa; h_{up} is the thickness of upper layer, m; h_l is the thickness of lower layer, m.

Compression ratio of the separator layer between lower layer and stabilized base is defined as:

$$C_f = \frac{2{,}4 \cdot E_l E_f E}{E \cdot (h_l E_f + h_f E_l) + 2{,}4 \cdot E_l E_f h \mu_1}, \quad (14)$$

where: E_l is the elasticity modulus of lower layer, MPa; h_l is the thickness of lower layer, m; E_f is the elasticity modulus of stabilized base, MPa; h_f is the thickness of stabilized base, m.

The separator layer is proposed to model by FE 262 of the program LIRA finite element library. Finite ele-

ments FE 262 model the separate layer as independent axial springs which have stiffness in the vertical direction Z only.

Two-layer rigid pavement with the separator layer and stabilized base is shown in Fig. 3.

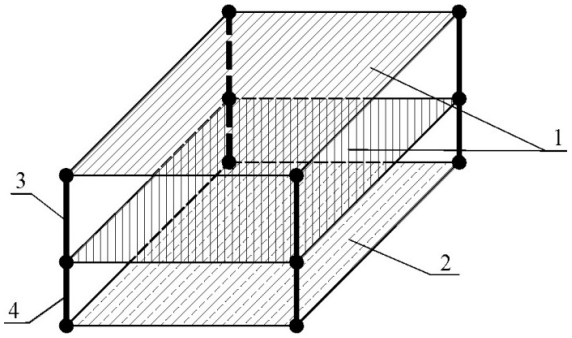

Fig. 3. Finite element model of two-layer rigid pavement: *1* – shell finite element that models upper and lower concrete slabs; *2* – shell finite element on a Winkler foundation that models stabilized base; *3* – finite element FE 262 that models the separator layer between upper and lower concrete slab; *4* – finite element FE 262 that models the separator layer between lower concrete slab and stabilized base

The stiffness values assigned to each node, *R* (stiffness of FE 262 of the program LIRA finite element library), are determined based upon the area that contributes to the stiffness of the node. For equally spaced nodes of shell finite element mesh, the nodes may be categorized into one of four types: interior nodes, edge nodes and corner nodes. Based upon the concepts of contributing area, the stiffness of the interior nodes *R* must be twice that of the edge nodes R_e; the stiffness of the edge nodes R_e must be twice that of the corner nodes R_c.

The stiffness of FE 262 between upper and lower layers of rigid pavement is defined by the relationship:

$$R_p = \frac{C_p LB}{(n_p - 1)(n_K - 1)}, \quad (15)$$

where: L is the slab length, m; B is the slab width, m; n_r is the number of node rows in slab finite element model; n_k is the number of node columns in slab finite element model.

The stiffness of FE 262 between upper and lower layers of rigid pavement is defined as:

$$R_f = \frac{C_f LB}{(n_p - 1)(n_K - 1)}. \quad (16)$$

For unequally spaced nodes in a shell finite element model the stiffness of the interior nodes *R* is defined as

$$R = \frac{C(a_1 b_1 + a_2 b_1 + a_1 b_2 + a_2 b_2)}{4}, \quad (17)$$

where: a_1, a_2, b_1, b_2 are spaces between nodes as shown in Fig. 4.

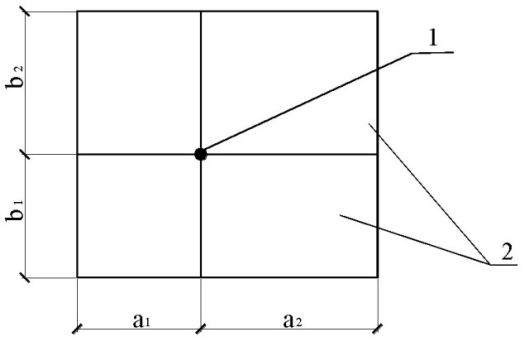

Fig. 4. Scheme for the FE 262 stiffness determining (case of unequally spaced nodes): 1 – interior node, 2 – shell finite element

If the separator layer is not located between rigid pavement layers compression ratio is defined by (Totskyi *et al.* 1982):

$$C_i' = \frac{2{,}4 \cdot E_i E_{i+1}}{(h_i E_{i+1} + h_{i+1} E_i)}, \quad (18)$$

where: E_i, E_{i+1}, h_i, h_{i+1} are the same as in equation (11).

For two-layer rigid pavement equation (18) is as follow:

$$C_p' = \frac{2{,}4 \cdot E_{up} E_l}{h_{up} E_l + h_l E_{up}}, \quad (19)$$

where: E_{up}, E_l, h_{up}, h_l are the same as in equation (13).

Compression ratio of the separator layer between lower layer and stabilized base is defined as:

$$C_f' = \frac{2{,}4 \cdot E_l E_f}{h_l E_f + h_f E_l}, \quad (20)$$

where: E_l, h_l, E_f, h_f are the same as in equation (14).

The stiffness of FE 262 between upper and lower layers of rigid pavement without the separator layer is as follow:

$$R_p' = \frac{C_p' LB}{(n_p - 1)(n_K - 1)}, \quad (21)$$

where: L, B, n_r, n_k are the same as in equation (15).

The stiffness of FE 262 between upper and lower layers without the separator layer is defined as:

$$R'_f = \frac{C'_f LB}{(n_p - 1)(n_K - 1)}. \quad (22)$$

For unequally spaced nodes in a shell finite element model the stiffness of the interior nodes R is defined by the relationship:

$$R = \frac{C'(a_1 b_1 + a_2 b_1 + a_1 b_2 + a_2 b_2)}{4}, \quad (23)$$

where: a_1, a_2, b_1, b_2 are the same as in equation (17).

4. Finite element results

This part presents some typical results from the finite element rigid pavement model. All of the solutions presented in the following part were computed on program LIRA.

Edge loading of the four–wheel B–747–400ER, B–787–9, B–747–8 main gears (Table 1) was analyzed for the following case: 450-mm upper PCC slab (7,5- by 7,5-m. slab dimensions, E =35300 MPa), 300-mm lower lean concrete slab (E = 17000 MPa), stabilized base (E = 7800 MPa), and Winkler foundation (K = 60 MN/m^3). The separator layer is located between rigid pavement layers.

Table 1. Four-wheel main landing gears

Aircraft	B–747–400ER	B–787–9	B–747–8
Magnitude of the main gear static load	969,0 kN	1167,8 kN	1053,6 kN
Main gear tire pressure	1,580 MPa	1,558 MPa	1,554 MPa
Magnitude of the wheel load with dynamic ratio (SNiP)	314,93 kN	379,54 kN	342,42 kN

The finite element mesh for the B–787–9 problem is shown in Fig. 5. Wheel load was modeled as square load that has the same magnitude as the nominal tire contact area.

The two-layer rigid pavement was also calculated by using the State norms of Ukraine (SNiP 2.05.08–85). The bending moment is determined on the upper and lower slab. The maximum bending moment of upper slab is labeled as M_{up}, the maximum bending moment of lower slab is labeled as M_l. The results obtained in the analysis are summarized in Table 2.

The maximum bending moment of upper slab computed by LIRA is more than the bending moment computed by SNiP but the maximum bending moment of lower slab computed by LIRA is less than the bending moment computed by SNiP. These finite element results coincide with conclusions of PhD N.B. Vasyliev (Vasyliev 2001).

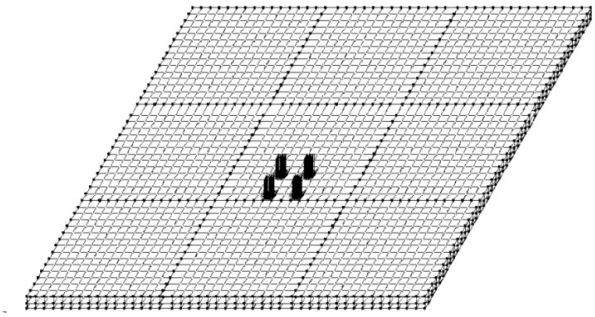

Fig. 5. Finite element model of the two-layer rigid pavement under impact of four-wheel B-787-9 main landing gear

Table 2. Comparative results of finite element and the State norms analysis

Aircraft	B–747–400ER	B–787–9	B–747–8
M_{up} (LIRA)	100,18 kN•m/m	103,06 kN•m/m	103,54 kN•m/m
M_{up} (SNiP)	97,80 kN•m/m	99,60 kN•m/m	101,40 kN•m/m
Δ_{up}	2,4%	3,5%	2,1%
M_l (LIRA)	12,34kN•m/m	12,63kN•m/m	13,01kN•m/m
M_l (SNiP)	13,95kN•m/m	14,20kN•m/m	14,50kN•m/m
Δ_l	–11,5%	–11,1%	–10,2%

Multi-slab jointed two-layer rigid pavement model allows analyzing the impact of all main landing gears of new large aircrafts such as A380. Nine-slab and twelve-slab jointed two-layer rigid pavement models for A380 problem are shown in Fig. 6, 7.

The finite element mesh for the A380 problem is shown in fig. 8. Impact of aircraft all main landing gears is not supported by the State norms (SNiP) method.

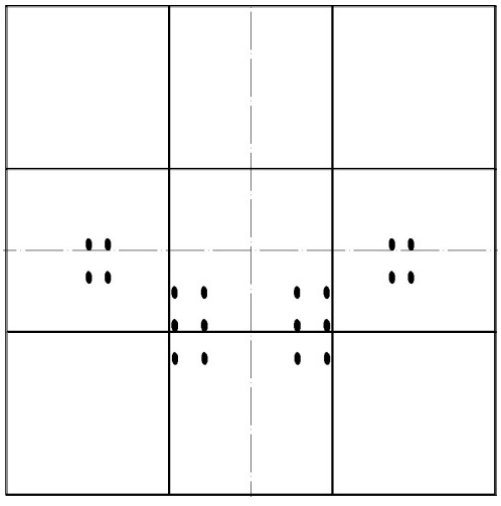

Fig. 6. Nine-slab geometry and load position for the A380 gears

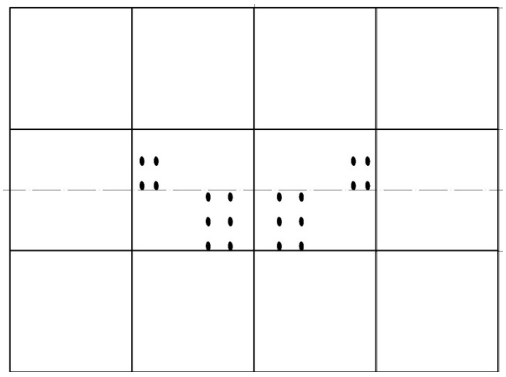

Fig. 7. 12-slab geometry and load position for the A380 gears.

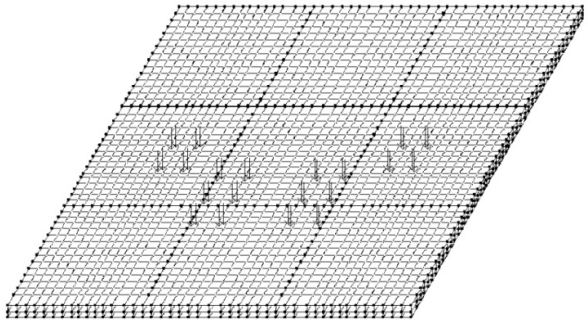

Fig. 8. Finite element model of the two-layer rigid pavement under impact of A380 all main landing gears.

Conclusions

Finite element model of multi-slab jointed two-layer rigid pavement was developed for program LIRA by author. Compression ratio relationships of Totskyi were applied to the LIRA finite element FE 262 stiffness calculation.

Sample numerical computations were performed using the introduced finite element model in program LIRA. Numerical solutions were compared to other solutions using the State norms method and N.B. Vasyliev approach.

The introduced finite element model provides a practical approach of computing multi-slab jointed two-layer rigid pavement in the general purpose program LIRA and takes into account such factors as multiple-wheel interaction, finite slab size, multiple-layer construction, variable joint stiffness and separator layer between upper and lower PCC slab. The using of research results will have to improve airfield rigid pavement design.

References

Brill, D. R. 1998. *Development of Advanced Computational Models for Airport Pavement Design*, Final Report DOT/FAA/AR-97/47, FAA. 89 p. Available from Internet: <http://www.tc.faa.gov/its/worldpac/techrpt/ar97-47.pdf>

Hammons, M. I. 1998. *Advanced Pavement Design: Finite Element Modelling for Rigid Pavement Joints*, Report II – Model Development, Report No. DOT/FAA/AR-97/7, FAA. 180 p. Available from Internet: <http://www.tc.faa.gov/its/worldpac/techrpt/ar9870.pdf>

Roesler J.; Evangelista F.; Domingues M. 2007. Effect of Gear Positions on Airfield Rigid Pavement Critical Stress Locations, *2007 FAA Airport Technology Transfer Conference*, April, 2007, Atlantic City, New Jersey, USA. Available from Internet: <http://www.ceat.uiuc.edu/PUBLICATIONS/presentations/ROESLER%20Rigid_PCC_stresses_Roesler.pdf>

Totskyi O. N.; Bezelyanskyi V. B.; Taruntaeva O. G. 1982. *Recomendatsyi po raschety mnogosloinykh pokrytyi aerodromov*. Moskwa. 56 p. (in Russian).

Vasyliev N. B. 2001. Perspectivy stroitelstva na aerodromakh monolitnykh tsementobetonnykh pokrytyi, *Aeroporty. Progressivnye tekhnologii* (4): 6-8.